http://dx.doi.org/10.5012/bkcs.2013.34.3.721

Multiple Nonenzymatic Labels-Based Impedimetric Aptamer Sensor for the Competitive Detection of Thrombin

Bongjin Jeong,[†] Rashida Akter,[‡] Oc Hee Han,[†,§] Choong Kyun Rhee,[†,§] and Md. Aminur Rahman[†,*]

[†]*Graduate School of Analytical Science and Technology (GRAST) and* [‡]*Chemistry Department, Chungnam National University, Daejeon 305-764 Korea.* [*]*E-mail: marahman@cnu.ac.kr*

[§]*Analysis Research Division, Daegu Center, Korea Basic Science Institute, Daegu 702-701, Korea*

Received December 8, 2012, Accepted December 27, 2012

Key Words : Gold nanoparticles, Multiple Nonenzymatic Labels, Impedance, Aptamer, Thrombin

Thrombin (TB) is a coagulation and serine protease that converts soluble fibrinogen to insoluble strands of fibrin as well as catalyzing many other coagulation-related reactions responsible for blood clotting. It plays an important role in thrombosis and haemostasis and its detection is very useful for early diagnosis of intracerebral hemorrhage[1] and pulmonary metastasis.[2] It is not present in blood under normal condition but can be elevated at low-micromolar concentrations during coagulation process.[3] Thus, the development of a high sensitive aptamer sensor for the detection of thrombin would be of great interest.

Many efforts have been devoted for developing novel aptamer sensors, which are based on fluorescence,[4] surface enhanced Raman spectroscopy,[5] surface plasmon resonance,[6] quartz crystal microbalance,[7] and electrochemistry.[8,9] Among these, electro-chemical methods are more advantageous due to simplicity, high sensitivity, fast response, low-cost, and miniaturization. In electrochemical methods, non enzymatic redox labels such as, methylene blue (MB)[10] and ferrocene[11] are commonly used for the fabrication of sensitive electrochemical thrombin aptamer sensors using voltammetric techniques. On the other hand, electrochemical impedance spectroscopy (EIS) is a powerful technique for the aptamer-based label-free detection of TB.[12,13] In particular, EIS-based thrombin aptamer sensor using multiple redox labels are promising for the detection of thrombin. For amplifying the response, coupling of nanomaterials such as multi walled carbon nanotube (CNT),[14] gold nanoparticles (AuNPs),[15] and quantum dot (QD)[8] have been used for the high sensitive aptamer-based thrombin detection. However, nanoparticle-coupled impedimetric thrombin aptamer sensor based on multiple labels for the amplified thrombin detection has not yet been studied.

In the present study, we have fabricated an impedimetric aptamer sensor based on gold nanoparicles (AuNPs) deposited polydopamine (PD/AuNPs) and AuNPs-supported multiple redox labels (TB/AuNPs/MB) for the amplified detection of thrombin. Figure 1 shows the schematic illustration of the aptamer sensor. The aptamer sensor was fabricated by immobilizing a thiolated aptamer (5'-SH, GGT TGG TGT GGT TGG-3') onto an AuNPs deposited PD film.

At first, a PD film was chemically grown on the Au electrodes by dropping a 10 mM of dopamine solution in 10 mM

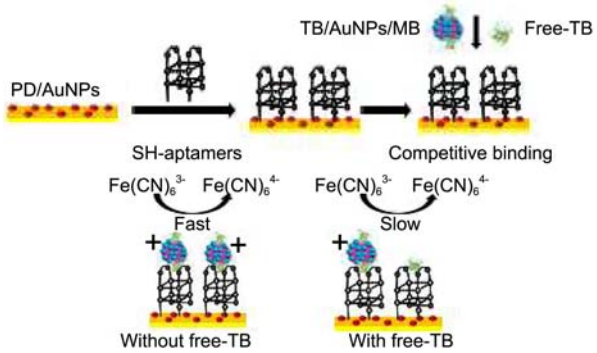

Figure 1. Schematic illustration of the fabrication of TB aptamer sensor (top) and the sensing principle (bottom).

Trizma ($NH_2C(CH_2OH)_3$·HCl (Tris) buffer at pH 8.5[16] and kept the electrode for 18 h in room temperature. After drying the Au/PD electrdoe, it was incubated in a colloidal solution of AuNPs (diameter 4-5 nm, Sigma Co.) for 12 h in order to deposit AuNPs on the PD film. On the other hand, TB/AuNPs/MB was prepared by firstly incubating 1.0 mL of AuNPs in a 10 mM *N*-2-hydroxyethylpiperazine-*N*′-2-ethanesulfonic acid (HEPES) solution (pH 7.4) containing 0.2 nM TB for 1 h at room temperature for partly covering the AuNPs surface with TB. The TB/AuNPs conjugates were formed through the interaction between amine groups and of TB and AuNPs. After removing the free TB and AuNPs by centrifugation, the TB/AuNPs conjugate was then incubated in a 5.0 mM MB solution for 12 h. MB was attached on the bare surface of AuNPs through the charge interaction between the positive charges of TB and the negative charges of AuNPs.

In Figure 2, the PD/AuNPs film and TB/AuNPs/MB conjugate were characterized using scanning electron microscopy (SEM), dynamic light scattering (DLS), and field emission transmission electron microscopic (FE-TEM) techniques. For the PD/AuNPs film, SEM images (Figure 2(a) and 2(b)) show that the PD surface mostly covered by AuNPs, which allows more immobilization of aptamer. For the PD/AuNPs/MB conjugate, the hydrodynamic size of AuNPs (~9 nm) increased after conjugation with TB and MB (~12 nm) as shown in DLS spectra (Figure 2(c)). FE-TEM images (inset of Figure 2(d)) show that the size of the AuNPs was about 5

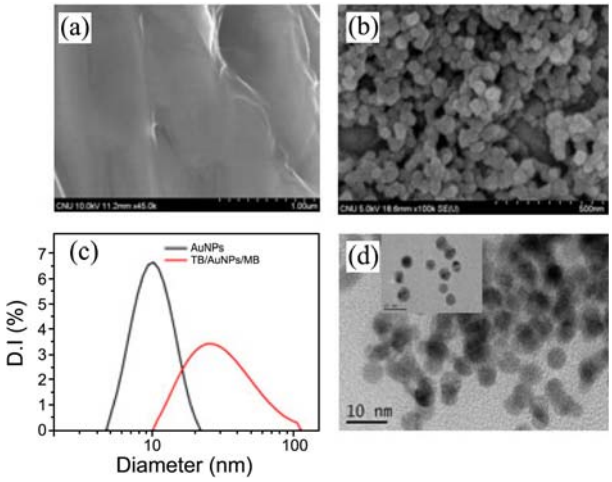

Figure 2. SEM images of (a) PD and (b) PD/AuNPs electrode, (c) DLS and (d) FE-TEM images of AuNPs and TB/AuNPs/MB conjugate.

nm and they are separately distributed. The size of the TB/AuNPs/MB conjugate was found to be increased than the size of bare AuNPs, which was found to be aggregated (Figure 2(d)).

The thrombin detection is based on the competitive binding between MB-conjugated TB (TB/AuNPs/MB) and free-thrombin for the active binding sites of aptamer. After competitive binding for 12 h, impedance measurements were carried out in a 1.0 mM of $[Fe(CN)_6]^{3-/4-}$ solution at 0.2 V (*vs*. Ag/AgCl) with the frequency range between 0.01 Hz-100 kHz. The TB/AuNPs/MB conjugate acted as the amplifying probe, where MB is a positive charged electroactive marker that facilitates the electron transfer of the negative charged $Fe(CN)_6]^{3-/4-}$ ions. Thus, the electron transfer resistances (ΔR_{ET}), which are determined from the diameter of the semi-circle in the Nyquist plot are increased after competitive binding. The ΔR_{ET} values between before and after competitive binding increased with increasing concentration of free-TB. The linear relationship between ΔR_{ET} and TB concentration is observed and thus, TB detection is possible with the proposed aptamer sensor.

Figure 3(a) shows the Nyquist plots obtained in a $[Fe(CN)_6]^{3-/4-}$ solution before and after competitive binding between conjugated- and free-TB. In the absence of free-TB, the aptamer probe only interacts with the conjugate. Thus, the Nyquist plot shows a small semi-circle corresponding to a low R_{ET} value. In the presence of both free- and conjugated-TB in the binding solution (HEPES buffer), some amount of free-TB bounds with the aptamer probe, which results in a decrease in the amount of positive charged MB at the aptamer probe. As a result, the electron transfer process of $Fe(CN)_6]^{3-/4-}$ is slowed down and the Nyquist plot shows relatively bigger semi-circle. With increasing concentration of free-TB in the binding solution, the diameters of semi-circle are increased. Figure 3(b) shows the calibration plot by using the ΔR_{ET} value obtained from the diameters of the semi-circles for various concentrations of free-TB. The linear range was determined as 0.01-1.4 nM. The linear dependence

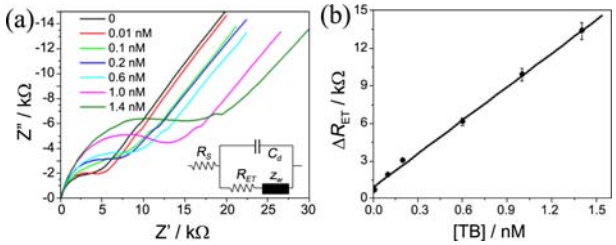

Figure 3. (a) Nyquist plots obtained in a $[Fe(CN)_6]^{3-/4-}$ solution. Inset shows an equivalent circuit. (b) Corresponding calibration plot of ΔR_{ET} *vs*. [TB].

between ΔR_{ET} and concentration of free-TB yielded a regression equation of ΔR_{ET} (kΩ) = (0.94 ± 0.16) + (8.92 ± 0.21) [TB] (nM) with a correlation co-efficient of 0.998. The detection limit is determined to be 0.01 nM (10 pM), which is much lower than those reported for other reported impedance-based aptamer sensors.[6,13,17,18]

In summary, an impedimetric TB aptamer sensor based on multiple non enzymatic labels has been fabricated. The results show that the multiple non-enzymatic labels amplified the sensitivity of the TB detection.

Acknowledgments. This research was supported by a research grant from Chungnam National University (grant no. 2011-0716).

References

1. Hu, S.; Xi, G.; Jin, H.; He, Y.; Keep, R. F.; Hua, Y. *Brain Res.* **2011**, *18*, 60.
2. Nierodzik, M. L.; Karpatkin, S. *Cancer Cell* **2006**, *10*, 355.
3. Bichler, J.; Heit, J. A.; Owen, W. G. *Thrombosis Research* **1996**, *84*, 289.
4. Stojanovic, M. N.; Prada, D. P.; Landry, D. W. *J. Am. Chem. Soc.* **2001**, *123*, 4928.
5. Cho, H. S.; Baker, B. R.; Pagva, C. V.; Laurence, T. A.; Lane, S. M.; Lee, L. P. *Nano Lett.* **2008**, *8*, 4386.
6. Radi, A. E.; Sanchez, J. L. A.; Baldrich, E.; O'Sulivan, C. K. *Anal. Chem.* **2005**, *77*, 6320.
7. Bang, G. S.; Cho, S. Y.; Kim, B. G. *Biosens. Bioelectron.* **2005**, *21*, 863.
8. Hansen, J. A.; Wang, J.; Kawde, A.; Xiang, Y.; Gothelf, K. V.; Collins, G. *J. Am. Chem. Soc.* **2006**, *128*, 2228.
9. Willner, I.; Zayats, M. *Angew. Chem. Int. Ed.* **2007**, *46*, 6408.
10. Xiao, Y.; Piorek, B. D.; Plaxco, K. W.; Heeger, A. A. *J. Am. Chem. Soc.* **2005**, *127*, 17990.
11. Rahman, M. A.; Son, J. I.; Won, M.-S.; Shim, Y.-B. *Anal. Chem.* **2009**, *81*, 6604.
12. Xu, H.; Gorgy, K.; Gondran, C.; Goff, A. L.; Spinelli, N.; Lopez, C.; Defrancq, E.; Cosnier, S. *Biosens. Bioelectron* **2013**, in press.
13. Li, L. D.; Zhao, H. T.; Chen, Z.-B.; Mu, X.- J.; Guo, L. *Sens. Actuators B* **2011**, *157*, 189.
14. Kara, P.; de la Escosura-Muniz, A.; Maltez-da Costa, M., Guix, M.; Ozsoz, M.; Merkoci, A. *Biosens. Bioelectron.* **2010**, *26*, 1715.
15. Kwon, D.; Jeong, H.; Chung, B. H. *Biosens. Bioelectron.* **2011**, *28*, 454.
16. Lee, H.; Dellatore, S. M.; Miller, W. M.; Messersmith, P. B. *Science* **2007**, *318*, 426.
17. Li, X. X.; Shen, L. H.; Zhang, D. D. *Biosens.Bioelectron.* **2008**, *23*, 1624.
18. Cai, H.; Lee, T. M. H.; Hsing, I. M. *Sens. Actuators B* **2006**, *114*, 433.